

Heavily obscured AGN with BeppoSAX, INTEGRAL, SWIFT, XMM and Chandra: prospects for Simbol-X

R. Della Ceca¹, P. Severgnini¹, A. Caccianiga¹, A. Comastri², R. Gilli², F. Fiore³, E. Piconcelli³, P. Malaguti⁴, and C. Vignali^{5,2},

¹ Istituto Nazionale di Astrofisica – Osservatorio Astronomico di Brera, Milano, Italy

² Istituto Nazionale di Astrofisica – Osservatorio Astronomico di Bologna, Italy

³ Istituto Nazionale di Astrofisica – Osservatorio Astronomico di Roma, Italy

⁴ Istituto Nazionale di Astrofisica – IASF, Bologna, Italy

⁵ Dipartimento di Astronomia, Università di Bologna, Italy

Abstract. According to the latest versions of synthesis modeling of the Cosmic X-ray Background, Compton Thick AGN should represent $\sim 50\%$ of the total absorbed AGN population. However, despite their importance in the cosmological context, only a few dozens of Compton Thick AGN have been found and studied so far. We will briefly review this topic and discuss the improvement in this field offered by the Simbol-X mission with its leap in sensitivity ($E > 10$ keV) of more than a factor 500 with respect to previous X-ray missions.

Key words. galaxies:active - galaxies: Seyfert - galaxies: nuclei - X-ray:galaxies - surveys

1. Introduction

Active Galactic Nuclei (AGN) emit over the entire electromagnetic spectrum and are widely believed to be powered by accretion of matter onto a Supermassive (millions to billions solar masses) Black Hole (SMBH; Rees 1984). It is now well established that the largest fraction of the AGN population is obscured by a large amount of cold matter around the Active Nuclei that does not permit a direct view to the central energy source. The identification of sources hosting such obscured accreting nuclei is a difficult task: in the opti-

cal domain the active nuclei appear very dim and their luminosity is comparable to that of their host galaxies (leaving very weak indications of the presence of an AGN), while in the X-ray band (up to 10 keV) their selection is difficult as even hydrogen column densities (N_H) of the order of 10^{22} - 10^{23} cm⁻² strongly reduce the flux from the nuclear source.

However, despite their elusiveness, obscured sources are fundamental for our understanding of the SMBHs history as the large majority of the energy density generated by accretion of matter in the Universe seems to takes place in obscured AGN (Fabian et al. 1998), as testified by the integrated energy density contained in the cosmic X-ray back-

Send offprint requests to: R. Della Ceca, E-mail: roberto.dellaceca@brera.inaf.it

ground (XRB; Gilli et al. 2007, Comastri et al., these proceedings). Even more important, the recent discovery of quiescent SMBH in the nuclei of non-active nearby galaxies with prominent bulges (Kormendy & Richstone 1995, Magorrian et al. 1998), along with the presence of scaling relations between the central BH mass and galaxy properties (e.g. bulge luminosity/mass and velocity dispersion, Ferrarese & Merritt 2000) strongly suggest that AGN are leading actors in the formation and evolution of galaxies and, in general, of cosmic structures in the Universe (see Begelman 2004 and references therein).

For absorbed AGN having column densities up to few times 10^{23} cm^{-2} XMM-Newton and *Chandra* have already produced (and are still producing) a wealth of useful data up to $\sim 10 \text{ keV}$ that can be used to evaluate their statistical properties as a function of cosmic time (e.g. La Franca et al. 2005, Mueller & Hasinger 2007, Della Ceca et al., in preparation). On the other hand, the situation is almost completely unconstrained for the absorbed sources having N_H in excess of $\sim 10^{24} \text{ cm}^{-2}$ (the so called Compton Thick AGN), when the matter is optically thick to Compton scattering. According to the latest versions of synthesis modeling of the XRB (Gilli et al. 2007), these sources should represent $\sim 50\%$ of the total absorbed AGN population but only a few dozens of them (mostly local) have been found and studied so far.

We will briefly review here what do we know about the Compton Thick AGN Universe and which is the improvement offered by the Simbol-X mission. A review of several aspects of the Compton Thick AGN field can be found in Comastri (2004). Throughout this paper we consider $(H_o, \Omega_M, \Omega_\Lambda) = (70, 0.3, 0.7)$.

2. The Compton Thick AGN Universe

The Compton Thick AGN may be separated into two classes. If the absorbing column density is below a few times 10^{24} cm^{-2} , a significant fraction of the the high energy ($E > 10 \text{ keV}$) photons can escape after one or more scatterings, allowing the nuclear source to be directly visible above 10 keV . In this case the source

is called mildly Compton Thick (a good example is NGC 4945, Guainazzi et al. 2000, see also section 3 for a typical X-ray spectrum). On the contrary, if the absorbing column densities is close or above 10^{25} cm^{-2} , then the X-ray photons cannot escape even in hard X-rays, being trapped in the matter, downscattered to lower energies and eventually destroyed by photoelectric absorption; the X-ray spectrum is hence depressed over the entire X-ray energy range. In this case the source is called heavily Compton Thick; a well known example is NGC 1068 (Matt et al. 1997). The presence of Compton thick matter may be inferred through indirect arguments, such as the presence of a strong Iron K_α line complex at $6.4 - 7 \text{ keV}$ and the characteristic reflection spectrum (having the emission peak above 10 keV). It is thus clear that hard X-ray data above 10 keV are fundamental to unveil and study Compton Thick AGN and to have a real and unbiased census of SMBH in the Universe.

Our present knowledge of the Compton Thick AGN universe is mainly based on few *bona fide* Compton Thick sources. In Table 1 we have reported all the 18 AGN so far identified as Compton Thick sources (to our knowledge) thanks to observations above 10 keV with *BeppoSAX*, *INTEGRAL*, *SWIFT/BAT* and *SUZAKU*¹; their position in the luminosity redshift plane is shown in Fig.1.

All the objects are at $z < 0.05$ and the large majority are relatively low luminosity ($< 10^{43} \text{ erg s}^{-1}$) sources, a clear consequence of the flux limit above 10 keV ($\sim 10^{-11} \text{ erg cm}^{-2} \text{ s}^{-1}$) of the X-ray missions carried out so far. Nine of the Compton Thick sources belong to well defined and complete samples selected above 10 keV (e.g. Sazonov et al. 2007, Beckmann et al. 2006, Bassani et al. 2006, Markwardt et al. 2005), while the remaining 9 sources come from specific pointed observations of objects selected at other wavelengths. Finally only 4 heavily Compton Thick AGN (NGC 1068, NGC 7674, NGC 3393 ed NGC 4939) have been detected so far above 10 keV .

¹ Table 1 and Table 2 are an updated version of the list of Compton Thick AGN discussed in Comastri (2004).

Table 1. *Bona fide* Compton Thick AGN detected above 10 keV^a

Name	z	Opt.Class.	N_H (10^{22} cm ⁻²)	$\text{Log} L_{10-40\text{keV}}^b$ erg s ⁻¹	$\text{Log} f_{2-10\text{keV}}$ erg cm ⁻² s ⁻¹	EW_{Fe} (eV)	Ref.
Circinus	0.0014	Sy2	430 ⁺⁴⁰ ₋₇₀	41.90	-10.85	2310 ⁺¹²⁰ ₋₂₆₀	6,2,3,4,7,24
M51	0.0015	LIN/Sy2	560 ⁺⁴⁰⁰ ₋₁₆₀	40.76	-12.47	900 ⁺⁴⁰⁰ ₋₃₀₀	19
NGC 4945	0.0019	LINER	220 ⁺³⁰ ₋₄₀	42.30	-11.27	~ 1300	12,3,2,4
NGC 1068	0.0038	Sy2	>1000	>41.71	-11.41	~ 3100	1,2,3,4,5,
NGC 3079	0.0038	LIN/Sy2	1000 ⁺¹⁰⁰⁰ ₋₅₃₀	42.10	-12.42	2400 ⁺²⁹⁰⁰ ₋₁₅₀₀	20
NGC 7582 ^c	0.0053	Sy2	160 ⁺⁹⁴ ₋₄₆	42.61	-10.71	570 ⁺⁵⁷⁰ ₋₁₂₀	22,10
SWIFT0601.9-8636	0.0062	Gal	101 ⁺⁵⁴ ₋₃₈	41.92	-11.96	1060 ⁺¹⁶⁰ ₋₁₆₀	25
ESO138-G01	0.0091	Sy2	~ 150	42.52	-11.74	1700 ⁺⁴⁸⁰ ₋₄₀₀	4,14
NGC 5728	0.0094	Sy2	210 ⁺²⁰ ₋₂₀	43.04	-11.82	1000 ⁺³⁰⁰ ₋₃₀₀	23, 10
NGC 4939	0.0104	Sy2	>1000	> 42.63	-11.85	480 ⁺⁴²⁰ ₋₂₁₀	21
NGC 3690	0.0110	HII	252 ⁺¹³⁹ ₋₅₆	42.84	-11.95	636 ⁺²³⁶ ₋₂₇₀	16,17
NGC 3281	0.0115	Sy2	196 ⁺⁵ ₋₅	43.17	-11.54	526 ⁺²⁷⁰ ₋₁₄₄	18,2,10
Tol 0109-383	0.0116	Sy2	350 ⁺¹⁸⁰ ₋₁₄₀	42.63	-11.80	~ 1360	13,14
NGC 3393	0.0125	Sy2	>1000	> 42.85	-12.41	1400 ⁺⁷⁰⁰ ₋₇₀₀	21,5
MKN 3	0.0134	Sy2	127 ⁺²⁴ ₋₂₂	43.51	-11.19	997 ⁺³⁰⁰ ₋₃₀₇	9,10,3,2,4,7
NGC 6240	0.0243	LINER	218 ⁺⁴⁰ ₋₂₇	44.26	-11.71	1580 ⁺³⁸⁰ ₋₃₅₀	7,8
NGC 7674	0.0289	Sy2	>1000	>43.34	-12.30	900 ⁺⁴⁷⁰ ₋₂₉₉	11
MKN 231	0.042	BAL QSO	~ 200	43.7-44.3	-12.15	~ 250	26

References: (1) Matt et al. (1997); (2) Sazonov et al. (2007); (3) Beckmann et al. (2006); (4) Bassani et al. (2006); (5) Levenson et al. (2006); (6) Matt et al. (1999); (7) Bassani et al. (1999); (8) Vignati et al. (1999); (9) Cappi et al. (1999); (10) Markwardt et al. (2005); (11) Malaguti et al. (1998); (12) Guainazzi et al. (2000); (13) Iwasawa et al. (2001); (14) Collinge & Brandt (2000); (15) Franceschini et al. (2000); (16) Della Ceca et al. (2002); (17) Ballo et al. (2004); (18) Vignali & Comastri (2002); (19) Fukazawa et al. (2001); (20) Iyomoto et al. (2001); (21) Maiolino et al. (1998); (22) Turner et al. (2000); (23) Comastri et al. (2007); (24) Iwasawa et al. (1997); (25) Ueda et al. (2007); (26) Braitto et al. (2004).

Table notes -

^a We have not considered here the Compton Thick AGN candidate IRAS 09104+4109 (a type 2 QSO at z=0.442). The Compton Thick nature of this object had been previously suggested (Franceschini et al. 2000) by a marginal ($\sim 2.5\sigma$) detection in the 15-50 keV energy range and recently re-discussed (and not confirmed) by Piconcelli et al. (2007) using XMM-Newton data;

^b The 10-40 keV luminosities have been computed assuming a power-law spectral model with photon index equal to 1.9 and, for the mildly Compton Thick AGN have been corrected for absorption. For the sources having $N_H \gtrsim 10^{25}$ cm⁻² this correction is not possible and the computed luminosities are a lower limit to the intrinsic ones;

^c This source has been recently investigated by Piconcelli et al. (2007b) using XMM-Newton data. The XMM-Newton spectrum of the nuclear source is very complex (a combination of a mildly absorbed, $N_H \sim 10^{24}$ cm⁻², power-law and a pure reflected component both obscured by a column density of $\sim 4 \times 10^{22}$ cm⁻²) also showing dramatic spectral changes.

At the few *bona fide* Compton Thick sources reported in Table 1 we may add the Compton Thick AGN *candidates*, for which we have observations only below 10 keV. From

these observations, the heavily absorbed active nature of these sources is suggested by the presence of a strong ($\text{EW} \gtrsim 500$ eV) Fe emission line, a characteristic property of

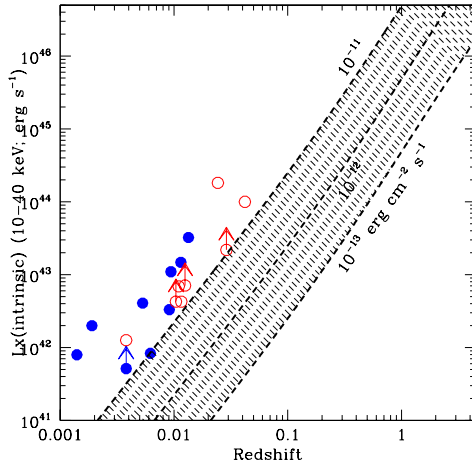


Fig. 1. Position in the luminosity-redshift plane of the 18 *bona fide* Compton thick AGN detected so far above 10 keV to our knowledge. The arrows mark the heavily Compton thick sources for which even the measured luminosity above 10 keV represents a lower limit to the intrinsic ones. The dashed lines represent the flux limit (10–40 keV energy band) of 10^{-11} , 10^{-12} and 10^{-13} $\text{erg cm}^{-2} \text{s}^{-1}$. The filled circles mark the objects belonging to complete and well defined survey programs, while the open circles mark the sources coming from pointed observations of objects selected at other energies. The shaded area enclose the discovery space offered by the Simbol-X mission regarding the spectral investigations of Compton Thick AGN (see section 3). For MKN 231 we have used a (10–40 keV) luminosity of 10^{-11} erg s^{-1} .

the Compton Thick AGN population. The Compton Thick AGN candidates identified so far in this way are reported in Table 2. We note that for these sources (almost all at very low redshift) we lack the coverage above ~ 10 keV, thus we are unable to confirm the presence of an absorption cut off in the hard X-ray domain; only a conservative lower limit on the intrinsic N_H and nuclear luminosity can be placed.

About 30–50 Compton Thick AGN candidate have been also selected in the Chandra deep fields on the basis of (poor quality) X-ray and optical data (e.g. Tozzi et al. 2006, Alexander et al. 2003) and a few objects have been selected using the Sloan Digital

Sky Survey (Vignali et al. 2006); a few other candidates have been recently selected using X-ray data combined with Spitzer data (e.g. Polletta et al. 2006, Daddi et al. 2007, Fiore et al. 2007). We stress again that also for the Compton Thick candidates from the Chandra Deep fields and/or from Spitzer the intrinsic absorption column density and the intrinsic luminosities are unconstrained.

3. The Simbol-X view of Compton Thick AGN

The Simbol-X mission ² is expected to have a leap in sensitivity in the 10–40 keV band of more than a factor 500 with respect to previous X-ray missions.

To evaluate the impact of this mission on the studies of Compton Thick AGN at cosmological distances we have run spectral simulations using the satellite configuration and response files as reported in the notes posted in <http://www.iasfbo.inaf.it/simbolx/faqs.php> (March 28th, 2007 version).

To this purpose we assumed an adequate template of Compton Thick AGN. The adopted spectral model was a combination of the following components: a) a primary power-law component filtered by an absorbing column density $N_H > 10^{24} \text{ cm}^{-2}$; b) a scattered component having a scattered efficiency of $\sim 1\%$; c) a reflected component which accounts for few percent of the total unabsorbed flux in the 2–10 keV energy range and d) an Iron line complex (Fe lines at 6.4 and 6.97 keV) having an observed EW ~ 1 keV and a line ratio fixed from the atomic physics. All these spectral components are commonly observed in Compton Thick AGN (e.g the recent SUZAKU observation of NGC 5728 discussed in Comastri et al. 2007).

In Fig. 2, 3, and 4 we report three simulations (100 ksec each) corresponding to a mildly Compton Thick AGN ($N_H \sim 3 \times 10^{24} \text{ cm}^{-2}$) having $f_{10-40\text{keV}} \sim 10^{-11}$, $\sim 10^{-12}$ and $\sim 10^{-13} \text{ erg cm}^{-2} \text{s}^{-1}$, while in Fig. 5 we show

² The Simbol-X mission and its main scientific objectives are discussed in the F. Ferrando and F. Fiore contributions at this meeting.

Table 2. Compton Thick AGN candidates detected below 10 keV

Name	z	Opt.Class.	N_H (10^{22} cm^{-2})	$\text{Log } f_{2-10\text{keV}}$ $\text{erg cm}^{-2} \text{ s}^{-1}$	$\text{Log } L_{2-10\text{keV}}^a$ erg s^{-1}	EW_{Fe} (eV)	Ref.
NGC 1386	0.0029	Sy2	>100	-12.62	39.65	2300^{+1500}_{-500}	5,2
NGC 5643	0.0039	Sy2	>1000	-11.95	40.57	1900^{+1400}_{-700}	5
NGC 1365 ^b	0.0055	Sy2	>100	-12.03	40.79	2100^{+2100}_{-300}	17
ESO 428.G14	0.0057	Sy2	>150	-12.42	40.44	1600^{+500}_{-300}	2
NGC 2273	0.0062	Sy2	>1000	-12.00	40.93	2490^{+800}_{-680}	5
NGC 5347	0.0078	Sy2	>100	-12.66	40.47	1300^{+500}_{-500}	2,13
IC 2560	0.0097	Sy2	>100	-12.44	40.88	3600^{+1500}_{-1500}	7
NGC 4968	0.0099	Sy2	>160	-12.82	40.51	3000^{+1200}_{-1000}	1
UGC 2456	0.0120	Sy2	90^{+60}_{-30}	-12.44	41.06	1000^{+300}_{-400}	1
IC 3639	0.0110	Sy2	>1000	-12.46	40.97	3200^{+980}_{-1740}	4
MKN 1210	0.0135	Sy2	>100	-11.89	41.72	820^{+360}_{-430}	6
NGC 5135	0.0137	Sy2	>100	-12.80	40.82	1700^{+800}_{-600}	1
NGC 591	0.0152	Sy2	>160	-12.70	41.01	2200^{+700}_{-600}	1
IC 4995	0.0161	Sy2	>160	-12.54	41.22	1700^{+700}_{-700}	1
UGC 1214	0.0172	Sy2	>160	-12.55	41.27	1300^{+500}_{-500}	1
NGC 6552	0.0262	SY2	>100	-12.22	41.97	~ 900	6,14
NGC 7212	0.0266	Sy2	>160	-12.16	42.04	900^{+200}_{-300}	1,2
MKN 266	0.0279	Sy2	>100	-12.25	41.99	~ 575	16
UGC 5101	0.0394	LINER	140^{+10}_{-20}	-12.21	42.34	410^{+270}_{-240}	8,9
IRAS 19254-7245	0.062	HII	>100	-12.62	42.33	2000^{+600}_{-600}	10
S5 1946+708	0.1010	NELG	>280	-12.28	43.11	1800^{+1200}_{-1100}	3
XID 2608	0.125	Sy2	>150	-13.29	42.29	792^{+1151}_{-493}	12
IRAS00182-7112	0.327	LINER	>100	-12.82	43.70	910^{+460}_{-460}	18
IRAS F15307+3252	0.93	Sy2/QSO2	>100	-13.46	44.01	>2000	11
CDFS 202	3.7	Sy2/QSO2	>1000	-14.56	43.85	1185^{+1195}_{-922}	15

References: (1) Guainazzi et al. (2005); (2) Levenson et al. (2006); (3) Risaliti et al. (2003); (4) Risaliti et al. (1999); (5) Maiolino et al. (1998); (6) Bassani et al. (1999); (7) Iwasawa et al. (2002); (8) Imanishi et al. (2003); (9) Ptak et al. (2003); (10) Braito et al. (2003); (11) Iwasawa et al. (2005); (12) Mainieri et al. (2006); (13) Risaliti et al. (1999b); (14) Reynolds et al. (1994); (15) Norman et al. (2002); (16) Risaliti et al. (2000); (17) Iyomoto et al. (1997); (18) Nandra & Iwasawa (2007).

Table notes – ^a Observed luminosity (i.e. not corrected for absorption); ^b According to Risaliti et al. (2005) this source shows rapid Compton-Thick/Compton-Thin transitions.

a 100 ksec Simbol-X simulation of a heavily Compton Thick AGN ($N_H > 10^{25} \text{ cm}^{-2}$) for which we see only the reflected component and the Fe line complex. These simulations are briefly discussed below along with some considerations.

3.1. $f_{10-40\text{keV}} \sim 10^{-11} \text{ erg cm}^{-2} \text{ s}^{-1}$

The simulation reported in Fig.2 corresponds to a Compton Thick AGN with a $L_{10-40\text{keV}} \sim 10^{45} \text{ erg s}^{-1}$ at $z \sim 0.2$. With a Simbol-X exposure of 100 ksec we should accumulate ~ 11000 net counts from the Macro Pixel Detector (MPD) and ~ 8000 net counts from the Cd(Zn)Te detector (CZT). The analysis of these data shows that the N_H will be deter-

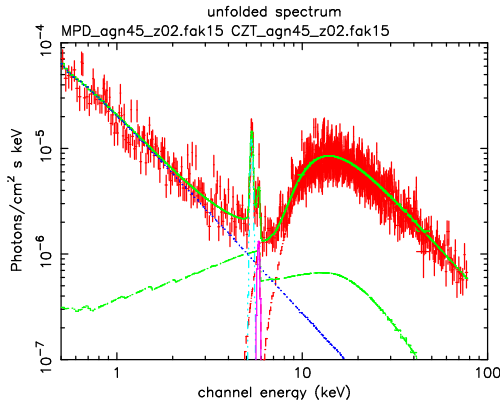


Fig. 2. Simulated 100 ksec Simbol-X observation for a midly Compton Thick AGN ($N_H \sim 3 \times 10^{24} \text{ cm}^{-2}$, spectral model as described in the text) with $f_{10-40\text{keV}} \sim 10^{-11} \text{ erg cm}^{-2} \text{ s}^{-1}$. In particular this simulation corresponds to a source with a $L_{10-40\text{keV}} \sim 10^{45} \text{ erg s}^{-1}$ at $z \sim 0.2$.

mined with an accuracy (90% confidence error) of $\sim 5\%$, while the intrinsic luminosity will be determined with an accuracy of $\sim 10\%$. Furthermore the positions and the normalizations of the Fe lines will be measured with an accuracy of few % and 15%, respectively.

We should be able to accumulate X-ray spectra of such a quality in the local Universe ($z < 0.02$) for Compton Thick AGN with $L_{10-40\text{keV}} \sim 10^{43} \text{ erg s}^{-1}$ and up to $z=0.2$ for Compton Thick AGN with $L_{10-40\text{keV}} \sim 10^{45} \text{ erg s}^{-1}$ (see the line corresponding to $\sim 10^{-11} \text{ erg cm}^{-2} \text{ s}^{-1}$ in Fig. 1). According to the CXB synthesis models (see Comastri et al., these proceedings) ~ 40 Compton Thick AGN at $|b| > 20^\circ$ above this flux limit are expected. Possible Simbol-X targets with this flux are obviously the well known Compton Thick AGN reported in Table 1 as well as Infrared Bright Local Galaxies, that can host Compton Thick AGN which are at the present optically elusive (so not identified yet, see e.g. the case of Arp 299, Della Ceca et al. 2002; Ballo et al. 2004).

3.2. $f_{10-40\text{keV}} \sim 10^{-12} \text{ erg cm}^{-2} \text{ s}^{-1}$

A 100 ksec simulation of a Compton Thick AGN with a $L_{10-40\text{keV}} \sim 10^{45} \text{ erg s}^{-1}$ at $z \sim$

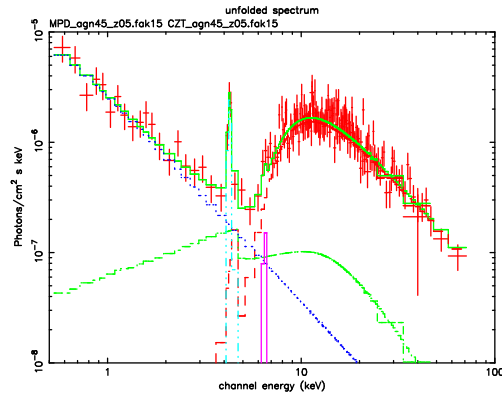


Fig. 3. As figure 2 but for one object having $f_{10-40\text{keV}} \sim 10^{-12} \text{ erg cm}^{-2} \text{ s}^{-1}$, corresponding to a source with a $L_{10-40\text{keV}} \sim 10^{45} \text{ erg s}^{-1}$ at $z \sim 0.5$.

0.5 is shown in Fig. 3 ($f_{10-40\text{keV}} \sim 10^{-12} \text{ erg cm}^{-2} \text{ s}^{-1}$). About ~ 1500 MPD net counts and ~ 800 CZT net counts will be accumulated allowing us to determine the N_H and the intrinsic luminosity with an accuracy of $\sim 10\%$ and $\sim 20\%$, respectively. The positions and the normalizations of the Fe lines will be measured with an accuracy of few % and $\sim 40\%$, respectively.

X-ray spectra of this quality are expected for Compton Thick AGN with $L_{10-40\text{keV}} \sim 10^{45} \text{ erg s}^{-1}$ up to $z \sim 0.5$, and according to the CXB synthesis modeling ~ 1500 Compton Thick AGN at $|b| > 20^\circ$ are expected above $\sim 10^{-12} \text{ erg cm}^{-2} \text{ s}^{-1}$. Possible Simbol-X targets are some of the candidate Compton Thick AGN listed in Table 2, Infrared Bright Local Galaxies and well known Ultra Luminous Infrared Galaxies (ULIRGS, see e.g. the case of IRAS 19254-7245, Braitto et al. 2003).

3.3. $f_{10-40\text{keV}} \sim 10^{-13} \text{ erg cm}^{-2} \text{ s}^{-1}$

A Compton Thick AGN with a $L_{10-40\text{keV}} \sim 10^{45} \text{ erg s}^{-1}$ at $z \sim 1.5$ should appear as shown in Fig. 4 ($f_{10-40\text{keV}} \sim 10^{-13} \text{ erg cm}^{-2} \text{ s}^{-1}$; ~ 350 MPD net counts; ~ 150 CZT net counts). The intrinsic N_H will be determined with an accuracy $\sim 20 - 40\%$, while the intrinsic luminosity will be determined within a factor 2.

A few million of Compton Thick AGN ($|b| > 20^\circ$) are expected at this flux limit

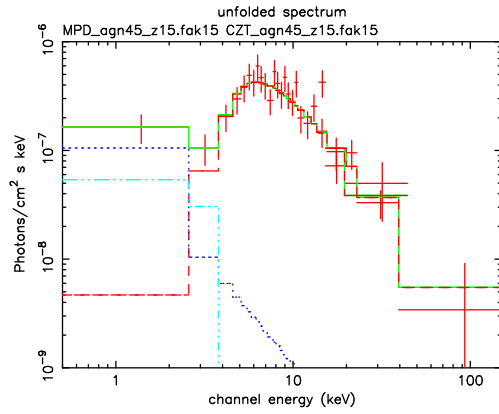


Fig. 4. As figure 2 but for one object having $f_{10-40\text{keV}} \sim 10^{-13} \text{ erg cm}^{-2} \text{ s}^{-1}$, corresponding to a source with a $L_{10-40\text{keV}} \sim 10^{45} \text{ erg s}^{-1}$ at $z \sim 1.5$.

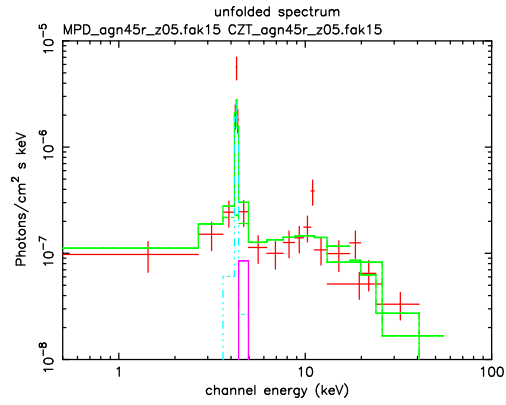


Fig. 5. Simulated 100 ksec Simbol-X observation for a heavily Compton Thick AGN (spectral model as described in the text) corresponding to a source with a $L_{10-40\text{keV}} \sim 10^{45} \text{ erg s}^{-1}$ at $z \sim 0.5$.

and possible Simbol-X targets are the candidate Compton Thick AGN selected from the Spitzer/Herschel surveys (e.g. Polletta et al. 2006, Daddi et al. 2007, Fiore et al. 2007) and some of the faintest ULIRGS.

3.4. Heavily Compton Thick AGN

Finally in Fig 5 we show a simulated 100 ksec Simbol-X spectrum for a heavily Compton Thick AGN corresponding to a source with an intrinsic luminosity $L_{10-40\text{keV}} \sim 10^{45} \text{ erg s}^{-1}$ at $z \sim 0.5$ ($f_{10-40\text{keV}} \sim 7 \times 10^{-14} \text{ erg cm}^{-2} \text{ s}^{-1}$; ~ 250 MPD net counts; ~ 100 CZT net counts). Deeply buried sources like NGC 1068 can be investigated up to cosmological distances.

4. Conclusions

The Compton Thick AGN universe is practically a new field in high energy astrophysics since very few Compton Thick AGN (mostly in the local Universe) have been found and studied so far. The Simbol-X mission, with its improved sensitivities above 10 keV with respect to previous satellites, is expected to open this field to detailed investigation up to cosmological distances ($z \sim 0.5 - 1.5$).

Acknowledgements. We thanks V. Braitto and L. Ballo for useful discussions. This work received par-

tial financial support from ASI, MIUR (PRIN 2006-02-5203) and INAF.

References

- Alexander, D. M., et al. 2003, *AJ*, 126, 539
- Ballo, L., Braitto, V., Della Ceca, R., Maraschi, L., Tavecchio, F., & Dadina, M. 2004, *ApJ*, 600, 634
- Bassani, L., Dadina, M., Maiolino, R., Salvati, M., Risaliti, G., della Ceca, R., Matt, G., & Zamorani, G. 1999, *ApJS*, 121, 473
- Bassani, L., Malizia, A., Stephen, J. B., & for the INTEGRAL AGN survey team 2006, *ArXiv Astrophysics e-prints*, arXiv:astro-ph/0610455
- Beckmann, V., Soldi, S., Shrader, C. R., Gehrels, N., & Produit, N. 2006, *ApJ*, 652, 126
- Begelman, M. C. 2004, *Coevolution of Black Holes and Galaxies*, 374
- Braitto, V., et al. 2003, *A&A*, 398, 107
- Braitto, V., et al. 2004, *A&A*, 420, 79
- Cappi, M., et al. 1999, *A&A*, 344, 857
- Collinge, M. J., & Brandt, W. N. 2000, *MNRAS*, 317, L35
- Comastri, A. 2004, *Supermassive Black Holes in the Distant Universe*, 308, 245
- Comastri, A., Gilli, R., Vignali, C., Matt, G., Fiore, F., & Iwasawa, K. 2007, *ArXiv e-prints*, 704, arXiv:0704.1253

- Daddi, E., et al. 2007, ArXiv e-prints, 705, arXiv:0705.2832
- Della Ceca, R., et al. 2002, ApJ, 581, L9
- Fabian, A. C., Barcons, X., Almaini, O., & Iwasawa, K. 1998, MNRAS, 297, L11
- Ferrarese, L., & Merritt, D. 2000, ApJ, 539, L9
- Fiore, F., et al. 2007, ArXiv e-prints, 705, arXiv:0705.2864
- Franceschini, A., Bassani, L., Cappi, M., Granato, G. L., Malaguti, G., Palazzi, E., & Persic, M. 2000, A&A, 353, 910
- Fukazawa, Y., Iyomoto, N., Kubota, A., Matsumoto, Y., & Makishima, K. 2001, A&A, 374, 73
- Gilli, R., Comastri, A., & Hasinger, G. 2007, A&A, 463, 79
- Guainazzi, M., Matt, G., Brandt, W. N., Antonelli, L. A., Barr, P., & Bassani, L. 2000, A&A, 356, 463
- Guainazzi, M., Matt, G., & Perola, G. C. 2005, A&A, 444, 119
- Imanishi, M., Terashima, Y., Anabuki, N., & Nakagawa, T. 2003, ApJ, 596, L167
- Iyomoto, N., Fukazawa, Y., Nakai, N., & Ishihara, Y. 2001, ApJ, 561, L69
- Iyomoto, N., Makishima, K., Fukazawa, Y., Tashiro, M., & Ishisaki, Y. 1997, PASJ, 49, 425
- Iwasawa, K., Fabian, A. C., & Matt, G. 1997, MNRAS, 289, 443
- Iwasawa, K., Matt, G., Fabian, A. C., Bianchi, S., Brandt, W. N., Guainazzi, M., Murayama, T., & Taniguchi, Y. 2001, MNRAS, 326, 119
- Iwasawa, K., Maloney, P. R., & Fabian, A. C. 2002, MNRAS, 336, L71
- Iwasawa, K., Crawford, C. S., Fabian, A. C., & Wilman, R. J. 2005, MNRAS, 362, L20
- Kormendy, J., & Richstone, D. 1995, ARA&A, 33, 581
- La Franca, F., et al. 2005, ApJ, 635, 864
- Levenson, N. A., Heckman, T. M., Krolik, J. H., Weaver, K. A., & Zdotycki, P. T. 2006, ApJ, 648, 111
- Magorrian, J., et al. 1998, AJ, 115, 2285
- Maiolino, R., Salvati, M., Bassani, L., Dadina, M., della Ceca, R., Matt, G., Risaliti, G., & Zamorani, G. 1998, A&A, 338, 781
- Mainieri, V., et al. 2006, ArXiv Astrophysics e-prints, arXiv:astro-ph/0612361
- Malaguti, G., et al. 1998, A&A, 331, 519
- Markwardt, C. B., Tueller, J., Skinner, G. K., Gehrels, N., Barthelmy, S. D., & Mushotzky, R. F. 2005, ApJ, 633, L77
- Matt, G., et al. 1997, A&A, 325, L13
- Matt, G., et al. 1999, A&A, 341, L39
- Mueller, A., & Hasinger, G. 2007, ArXiv e-prints, 708, arXiv:0708.0942
- Nandra, K., & Iwasawa, K. 2007, ArXiv e-prints, 708, arXiv:0708.0158
- Norman, C., et al. 2002, ApJ, 571, 218
- Piconcelli, E., Fiore, F., Nicastro, F., Mathur, S., Brusa, M., Comastri, A., & Puccetti, S. 2007, A&A, 473, 85
- Piconcelli, E., Bianchi, S., Guainazzi, M., Fiore, F., & Chiaberge, M. 2007b, A&A, 466, 855
- Polletta, M. d. C., et al. 2006, ApJ, 642, 673
- Ptak, A., Heckman, T., Levenson, N. A., Weaver, K., & Strickland, D. 2003, ApJ, 592, 782
- Rees, M. J. 1984, ARA&A, 22, 471
- Risaliti, G., et al. 1999, Memorie della Societa Astronomica Italiana, 70, 73
- Risaliti, G., Maiolino, R., & Salvati, M. 1999b, ApJ, 522, 157
- Risaliti, G., Gilli, R., Maiolino, R., & Salvati, M. 2000, A&A, 357, 13
- Risaliti, G., Woltjer, L., & Salvati, M. 2003, A&A, 401, 895
- Risaliti, G., Elvis, M., Fabbiano, G., Baldi, A., & Zezas, A. 2005, ApJ, 623, L93
- Reynolds, C. S., Fabian, A. C., Makishima, K., Fukazawa, Y., & Tamura, T. 1994, MNRAS, 268, L55
- Sazonov, S., Revnivtsev, M., Krivonos, R., Churazov, E., & Sunyaev, R. 2007, A&A, 462, 57
- Tozzi, P., et al. 2006, A&A, 451, 457
- Turner, T. J., Perola, G. C., Fiore, F., Matt, G., George, I. M., Piro, L., & Bassani, L. 2000, ApJ, 531, 245
- Ueda, Y., et al. 2007, ApJ, 664, L79
- Vignali, C., & Comastri, A. 2002, A&A, 381, 834
- Vignali, C., Alexander, D. M., & Comastri, A. 2006, MNRAS, 373, 321
- Vignati, P., et al. 1999, A&A, 349, L57